Synthesis and Micellization Behavior of Janus H-Shaped A_2BC_2 Terpolymers

Spiros Christodoulou, Paraskevi Driva, Hermis Iatrou, and Nikos Hadjichristidis*

Department of Chemistry, University of Athens, Panepistimiopolis, Zografou, 157 71 Athens, Greece

Received November 23, 2007; Revised Manuscript Received January 17, 2008

ABSTRACT: The synthesis of a series of H-shaped A_2BC_2 terpolymers (Janus-H terpolymers), where A is poly(dimethylsiloxane) (PDMS), B polybutadiene (PBd), and C polystyrene (PS), is presented. The synthetic approach involves (a) the selective reaction of lithium PDMS alkolate with the two chlorosilane groups of the heterofunctional linking agent [(chloromethylphenyl)ethyl]methyldichlorosilane (CMPEMDS) and (b) the linking reaction of the benzyl chloride group, which remained intact, with the living star $(PS)_2$PBd-DPHLi. The synthesis of the living miktoarm star is achieved by (a) the selective reaction of the PSLi chains with the two chlorines of the linking reagent 4-(dichloromethylsilyl)diphenylethylene (DCMSDPE), (b) the addition of *sec*-BuLi to the double bond of the DPE group, and (c) the polymerization of Bd, followed by end-capping of the living end with one monomeric unit of DPE. The micellization behavior of the Janus-H terpolymers was studied in methyl ethyl ketone, a selective solvent for the outer branches of the terpolymers, PS, and PDMS. The complexity of the architecture along with "microdomain segregation" phenomena, also observed, led to the formation of unimolecular micelles or micelles with very low degrees of association.

Introduction

Poly(dimethylsiloxane) (PDMS) is the most well-studied member of the polysiloxane family. As a result of its excellent thermal and oxidative stability, low absorption in UV, and good oxygen reactive ion etch resistance, PDMS is widely used in lithographic applications for microelectronics.[1] In addition, PDMS shows high flexibility, low glass transition temperature, low surface energy, and low solubility parameter. All these properties render PDMS-based materials very attractive in a variety of industrial areas. Therefore, the synthesis of well-defined dimethylsiloxane-based polymers with different architectures is of major importance for designing new materials.

Until now, anionic polymerization high-vacuum techniques combined with appropriate linking chemistry have been the most powerful tool for synthesizing complex macromolecular architectures. Unfortunately, anionic polymerization of hexamethylcyclotrisiloxane (D_3), the usual monomer of PDMS, suffers from backbiting reactions,[2,3] thus rendering the synthesis of PDMS-based polymers with complex macromolecular architectures difficult or even impossible. Recently, our group solved this problem by a two-step protocol[4] for the complete polymerization of D_3 without side reactions, and since then a few efforts in designing PDMS-based copolymers with complex macromolecular architecture were successfully accomplished.[4–7]

On the other hand, the micellization properties of linear block copolymers in selective solvents have attracted the attention of many research groups in the past few decades. It has been shown that the structural characteristics of the micelles are influenced by many factors such as chemical nature, molecular weights of blocks, concentration, temperature, and molecular architecture of the copolymer. A variety of techniques have been used for the determination of the molecular characteristics of the micelles, including low-angle and dynamic light scattering,[8–10] viscometry,[11,12] small-angle neutron scattering (SANS),[13] and small-angle X-ray scattering (SAXS).[14]

Although the molecular architecture can impose constraints that force the resulting aggregates to adopt different structural characteristics, only a few studies have systematically addressed this issue[15–18] due to the lack of well-defined materials.

In this study, a series of H-shaped A_2BC_2 terpolymers, where A is poly(dimethylsiloxane) (PDMS), B polybutadiene (PBd), and C polystyrene (PS), were successfully synthesized via anionic polymerization high-vacuum techniques and the combination of chlorosilane and benzyl chloride linking chemistry. This novel and general methodology is based on the linking reaction of in-chain benzyl chloride-functionalized PDMS {BzCl-$(PDMS)_2$} with the living center of $(PS)_2$PBd-DPHLi. The precursor BzCl-$(PDMS)_2$ was synthesized by the selective reaction of lithium PDMS alkolate with the chlorosilane group of ((chloromethyl)phenylethyl)dimethyldichlorosilane (CMPEMDS), leaving the benzyl chloride group intact.

In addition, the micellar behavior of the H-shaped terpolymers was studied by dynamic and static light scattering in methyl ethyl ketone (MEK), a selective solvent for PS and PDMS. Two of the samples formed unimolecular micelles, while one formed micelles with a very low aggregation number ($N_w = 2$). This result is attributed to the complexity of the architecture in combination with the incompatibility of the PS and PDMS branches in solution.

Experimental Section

Materials. Butadiene (Bd, Aldrich, 99%), styrene (S, Aldrich, 99%), isoprene (I, Aldrich, 99%), the solvents [tetrahydrofuran (THF), benzene, and hexanes, all reagent grade], the terminating agent (methanol), and trichloromethylsilane (Aldrich, >99%) were purified by high-vacuum techniques and standard procedures described in detail elsewhere.[19] Hexamethylcyclotrisiloxane (D_3, Aldrich, 99%) was melted, transferred into a flask, diluted with an equal volume of purified benzene, and stirred over CaH_2 overnight. The next day benzene and D_3 were distilled/sublimed into a flask containing polystyryllithium (PS^-Li^+), stirred for 3 h at room temperature, then distilled/sublimed into a cylinder, and finally split in precalibrated ampules. *sec*-Butyllithium (*sec*-BuLi) was prepared from *sec*-butyl chloride and lithium dispersion.[19] The heterofunctional linking agent, [(chloromethylphenyl)ethyl]methyldichlorosilane (CMPEMDS, ABCR, 99.9%), a mixture of *para* and *meta* isomers, was purified by fractional distillation in the vacuum line. It was then diluted with benzene and subdivided into ampules.

Methyltriphenylphosphonium iodide (Acros, 97%), *n*-BuLi (2.3 M in hexane, Aldrich), 4-bromobenzophenone (Aldrich, 98%), chloroform (Aldrich, 99.5%), and $MgSO_4$ were used as received.

* To whom correspondence should be addressed.

10.1021/ma702605w CCC: $40.75
Published on Web 03/05/2008

Scheme 1. General Reactions for the Synthesis of 4-(Dichloromethylsilyl)diphenylethylene

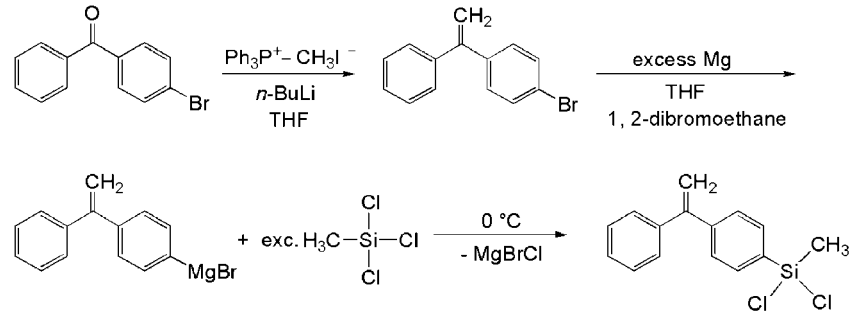

Scheme 2. General Reactions for the Synthesis of the Macromolecular Linking Agent BzCl-(PDMS)$_2$

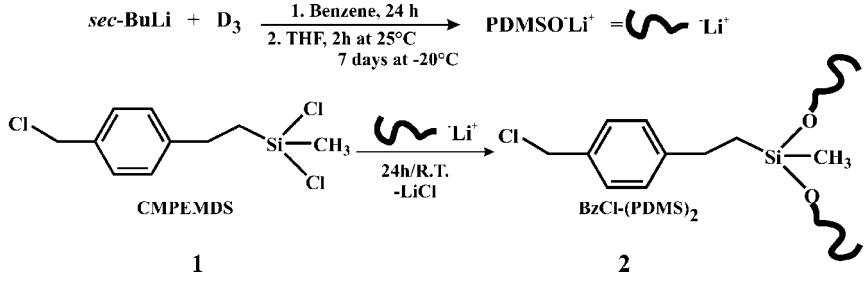

Scheme 3. General Reactions for the Synthesis of Janus-H Terpolymers, *j*-H

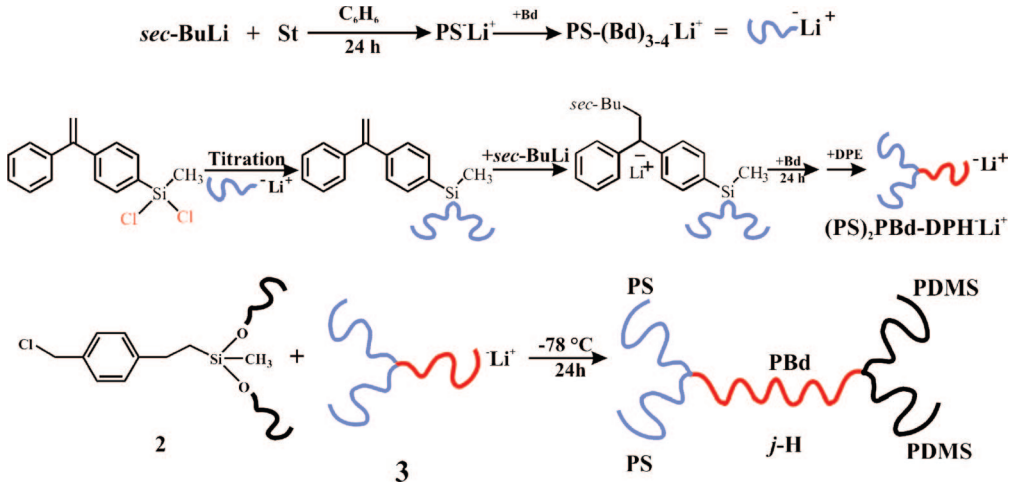

Magnesium turnings (Aldrich) were activated by sequential washings with 0.1 N HCl solution, distilled water, diethyl ether, and acetone and dried in a vacuum oven until constant weight.

Synthesis of 4-(Dichloromethylsilyl)diphenylethylene. 4-(Dichloromethylsilyl)diphenylethylene (DCMSDPE) was prepared from the Grignard reagent of 4-bromodiphenylethylene and trichloromethylsilane, using high-vacuum techniques and specially designed apparatuses. 4-Bromodiphenylethylene was obtained from the Wittig reaction of 4-bromobenzophenone and methyltriphenylphosphonium iodide in the presence of *n*-BuLi.[20] The route followed for the synthesis of DCMSDPE is given in Scheme 1. Full details of the synthetic procedure were presented in a previous paper.[21]

Synthesis of In-Chain Benzyl Chloride-Functionalized Poly(dimethylsiloxane) [BzCl-(PDMS)$_2$]. All synthetic manipulations were conducted with classic high-vacuum techniques. Polymerizations were carried out in evacuated, *n*-BuLi-washed, and solvent-rinsed glass reactors equipped with break-seals, for the addition of reagents and constrictions and for the removal of intermediate products. Full details of the used apparatus and techniques have been reported elsewhere.[19]

The synthetic approach of BzCl-(PDMS)$_2$ (Scheme 2) involves the selective replacement of the two chlorines ($-SiMeCl_2$) of CMPEMDS by PDMS chains, leaving the benzyl chloride group intact. A detailed synthetic procedure has been described previously.[6]

Synthesis of Janus H-Shaped Terpolymer Comprised of Two PDMS, Two PS Segments, and One PBd Segment. The synthetic strategy (Scheme 3) involves (i) the synthesis of the linking agent **2**, (ii) the synthesis of a living star copolymer **3**, and (iii) the linking reaction between **2** and **3**. As an example, the synthesis of *j*-H #2 [M_w(PS): 19.5K; M_n(PDMS): 19.2K; M_w(PBd): 19.5K] is given. The apparatus in Figure 1 was used for the synthesis of the living star. DCMSDPE (0.038 g, 1.3×10^{-1} mmol) was introduced into the main reactor after breaking the corresponding break-seal. A 10% solution of living polystyrene, end-capped with 2–3 monomeric units of butadiene ($M_w = 19.5$K, 6 g, 3.08×10^{-1} mmol) in benzene, prepared in a secondary reactor and connected to the apparatus, was added dropwise to the solution of DCMSDPE. The reaction was monitored by removing small aliquots (F) of the reacting solution and analysis by SEC. After 2 equiv of PS-(Bd)$_3^-$Li$^+$ (5.06 g, 2.6×10^{-1} mmol), relative to

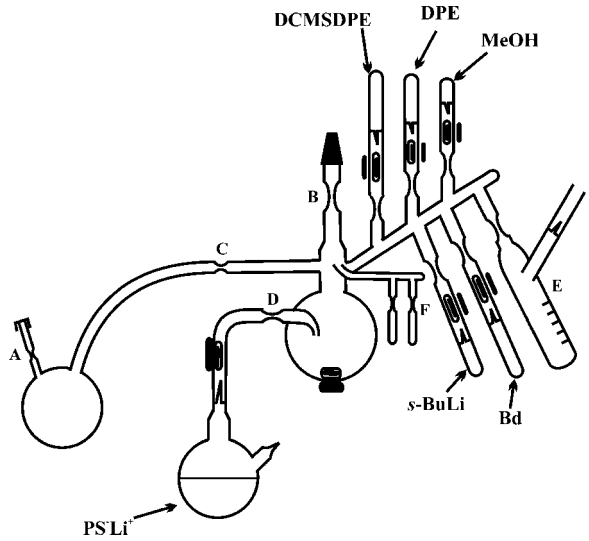

Figure 1. Apparatus for the synthesis of living stars.

DCMSDPE, were added to the reactor, and more importantly when the end point was confirmed by SEC, the titration was stopped. The flask containing the excess of the living PS solution (0.94 g, 0.48×10^{-1} mmol) was removed by heat-sealing (constriction D). The appropriate quantity of initiator *sec*-BuLi (1.3×10^{-1} mmol) was then added into the main reactor. The solution immediately turned deep red (addition of *sec*-BuLi to the double bond of the DPE group) and was left under stirring for 48 h. Butadiene (2.5 g) was then introduced into the main reactor, and the polymerization was allowed to proceed for 24 h. After the complete consumption of butadiene, the resulting living star was end-capped with DPE (2.6×10^{-1} mmol) at room temperature for 3 days. The produced starlike living copolymer (5.8 g (1×10^{-1} mmol)) was transferred into a volumetric ampule (E) and removed from the apparatus, while the remaining 1.76 g (3.03×10^{-2} mmol) was terminated with degassed methanol and kept for characterization/micellization study. The ampule (E) was then connected to a new reactor containing THF (150 mL) and equipped with ampules of the in-chain linking agent **2** (35 mL, 3.5 g, 9×10^{-2} mmol) and methanol. The temperature of THF was lowered to −78 °C, and the solutions of the living star and **2** were subsequently added and allowed to react overnight at −78 °C. The red color of the solution gradually faded to pink, which remained for ∼24 h, indicating the end of the linking reaction. The excess of the living star was terminated with degassed methanol, precipitated into an excess of methanol, and finally dried under vacuum to constant weight. The final product was obtained after fractionation with the toluene−hexane/methanol solvent/nonsolvent pair.

Molecular Characterization. The molecular weight distributions of the final and intermediate products were obtained by size exclusion chromatography (SEC), performed at 35 °C in two separate apparatuses. Both setups were equipped with a Waters model 510 pump, a Waters model 410 differential refractometer, and four Styragel (porosity range of 10^2-10^6 Å). The carrier solvent in one setup was THF and in the other chloroform/triethylamine (95/5 v/v) at a flow rate of 1.0 mL/min. In both cases calibrations were carried out with PS standards at a range of M_n from 1.5×10^3 to 9×10^5 g mol^{-1}.

Multidetector SEC analysis [size exclusion chromatography/refractive index (at 633 nm) and size exclusion chromatography/two-angle laser light scattering (SEC-TALLS) with laser power at 10 mW], using a Waters system equipped with a Waters 1525 high-pressure liquid chromatographic pump, Waters Ultrastyragel columns (HR-2, HR-4, HR-5E, and HR-6E), a Waters 2410 differential refractometer detector, and a Precision PD 2020 two-angle (15°, 90°) light scattering detector at 35 °C, was also performed to characterize the intermediate products. THF was used as an eluent at a rate of 1 mL/min.

The number-average molecular weights (M_n) of the final products were measured with a Jupiter model 231 recording membrane osmometer (MO) at 35 °C. Toluene, distilled from CaH_2 before use, was the solvent. The M_n values were obtained from the corresponding $(\pi/c)^{1/2}$ vs c plots, where π is the osmotic pressure and c is the concentration in g/mL. In all cases, the correlation coefficient was better than 0.99.

Nuclear magnetic resonance (NMR) spectra were generated with a Varian Unity Plus 300/54 instrument in $CDCl_3$ at room temperature.

Micellization Studies. Analytical grade MEK was dried over $MgSO_4$ by reflux for 24 h and was fractionally distilled with a Vigreux column just before use. Stock solutions were prepared by dissolving a weighted amount of sample in the appropriate volume of dried solvent with occasional stirring. All samples had dissolved in MEK after 24 h. The stock solutions were first heated at 60 °C for 2 h to ensure complete dissolution of the samples and removal of possible memory effects related to the formation of nonequilibrium structures. They were then left for 1 week to ensure the stability of the micelles formed. Solutions of lower concentration were obtained by subsequent dilution of the stock solutions. Before light scattering measurements the solutions were filtered through 0.45 μm nylon filters.

Static light scattering measurements were performed in MEK at 25 °C with a Chromatix KMX-6 low angle laser light scattering photometer, equipped with a 2 mW He−Ne laser operating at 633 nm. Apparent weight-average molecular weights, M_w, of the micelles and second virial coefficients, A_2, were obtained from the concentration dependence of the reduced scattering intensity according to eq 1

$$Kc/\Delta R_\theta = 1/M_{w,app} + 2A_2c + ... \quad (1)$$

where K is the combination of optical physical constants, including the differential refractive index increment, dn/dc, c is the concentration, and ΔR_θ is the difference between the Rayleigh ratio of the solution and the solvent.

The required refractive index increments, dn/dc, in MEK at 25 °C were determined with a Chromatix KMX-16 refractometer, operating at 633 nm and calibrated with aqueous NaCl solutions. The dn/dc value of narrow molecular weight PDMS samples in MEK, with a M_w close to that of the PDMS block, was equal to 0.02 mL g^{-1}. As a consequence, only PS (0.21 mL g^{-1}) and PBd (0.16 mL g^{-1}) parts have contributed to the apparent molecular weight of the micelle. The degree of association was determined by eq 2

$$N_w = M_{w,mic}/M_{w,(PS)_2PBd} \quad (2)$$

where $M_{w,mic}$ is the apparent molecular weight of PS/PBd parts of the micelle obtained by LALLS and $M_{w,(PS)_2PBd}$ the molecular weight of the intermediate miktoarm star copolymer, $(PS)_2PBd$, obtained by SEC-TALLS in a good solvent (THF).

Dynamic light scattering experiments were carried out with a Series 4700 Malvern system, composed of a PCS5101 goniometer with a PCS7 stepper motor controller, a Cyonics variable power Ar^+ laser, operating at 488 nm and with 10 mW power, a PCS8 temperature control unit, and a RR98 pump/filtering unit. A 192-channel correlator was used for accumulation of the data. Correlation functions were analyzed by the cumulant method and the Contin software provided by the manufacturer. Measurements were carried out at 45°, 60°, 75°, 90°, and 120°. The angular dependence of the ratio Γ/q^2, where Γ is the decay rate of the correlation function and q is the scattering vector, was negligible for the micellar solutions. Therefore, the measurements conducted at 90° were used. Measurements were performed starting at 25 °C and gradually increasing by 5° up to 50 °C. After each heating step, the solution was allowed to equilibrate for 20 min. Most of the measurements were performed in both a good (THF) and a selective solvent

(MEK) for comparison purposes. Apparent self-diffusion coefficients of the particles at zero concentration, $D_{0,app}$, were obtained by extrapolation to zero concentration using eq 3

$$D_{app} = D_0(1 + k_D c) \quad (3)$$

where D_{app} is the diffusion coefficient, measured at each concentration, and k_D the coefficient at the concentration dependence of D_{app}. Apparent hydrodynamic radii at infinite dilutions, R_h, were determined by eq 4

$$R_h = k_B T/6\pi\eta_0 D_{0,app} \quad (4)$$

where k_B is the Boltzmann constant, T the absolute temperature, and η_0 the viscosity of the solvent.

Results and Discussion

Polymer Synthesis. The general synthetic route followed for the synthesis of Janus H-shaped terpolymers is given in Scheme 3.

The methodology was based on (a) the recent advances in the controlled high-vacuum anionic polymerization of D_3, (b) the selectivity of the living PDMSOLi to the chlorosilane group of the heterofunctional linking agent CMPEMDS, and (c) the successful synthesis of a living star copolymer with the aid of the linking reagent DCMSDPE. The synthetic procedures were monitored by SEC. As an example, the SEC chromatograms obtained during the synthesis of *j*-H #2 are given in Figure 2.

The initial step of the synthesis involved the controlled polymerization of D_3 and linking reaction of the PDMSOLi with the chlorosilane group of CMPEMDS. A slight excess (~5%) of CMPEMDS over the living PDMSOLi was used to ensure complete linking. The selective reaction is based on the greater reactivity of the $-Si(Me)_2Cl$ than the $-CH_2Cl$ group toward silicon−oxygen nucleophiles.[22–24] The peak at lower elution volume (Figure 2a) corresponds to the in-chain linking agent BzCl-$(PDMS)_2$, which has double the molecular weight of the PDMS precursor, as expected. The absence of any peak, at even lower elution volume, excludes the formation of a 3-arm PDMS star homopolymer, indicating the selectivity of of PDMSOLi for $-Si(Me)_2Cl$.[23,24]

The synthesis of the living star copolymer **3** started with the titration of the two chlorine atoms of DCMSDPE with PS-$(Bd)_{2-3}^-Li^+$. The key factor for the synthesis of the in-chain DPE-PS is the faster reaction of the living PS with the chlorosilane group (nucleophilic substitution S_N) compared to the nucleophilic addition to the double bond of DCMSDPE. PSLi is end-capped with 2–3 monomeric units of Bd, before the linking reaction, in order to increase the selectivity for the chlorosilane groups.[25]

The titration lasted about 10 h, and almost 70% of the calculated polystyrene was added over the first 5 h. The linking reaction of the second arm was slower compared to the first one. The above is critical since any remaining −SiCl groups will react with the *sec*-BuLi added at the next step, while any remaining PS-$(Bd)_{2-3}^-Li^+$ will initiate the polymerization of butadiene.

The linking reaction was monitored by removing samples from the reactor and analyzing them by SEC. For a representative example see Figure 3. Initially, there was only one peak, corresponding to the product of DCMSDPE with one PS(I). As the titration proceeded, this peak decreased while that of the $(PS)_2$-D (II) increased. The disappearance of the peak corresponding to (I) indicated the end of the titration.

The reaction of *sec*-BuLi with the double bond of the DPE group of $(PS)_2$-D was confirmed by the immediate change of the solution color from pale yellow to deep red, indicative of the formation of DPELi. Here, it is also crucial to control the stoichiometry in order to avoid either the incomplete addition of *sec*-BuLi to the double bond (in the case of excess $(PS)_2$-D) or the reaction of any excess *sec*-BuLi with BzCl-$(PDMS)_2$.

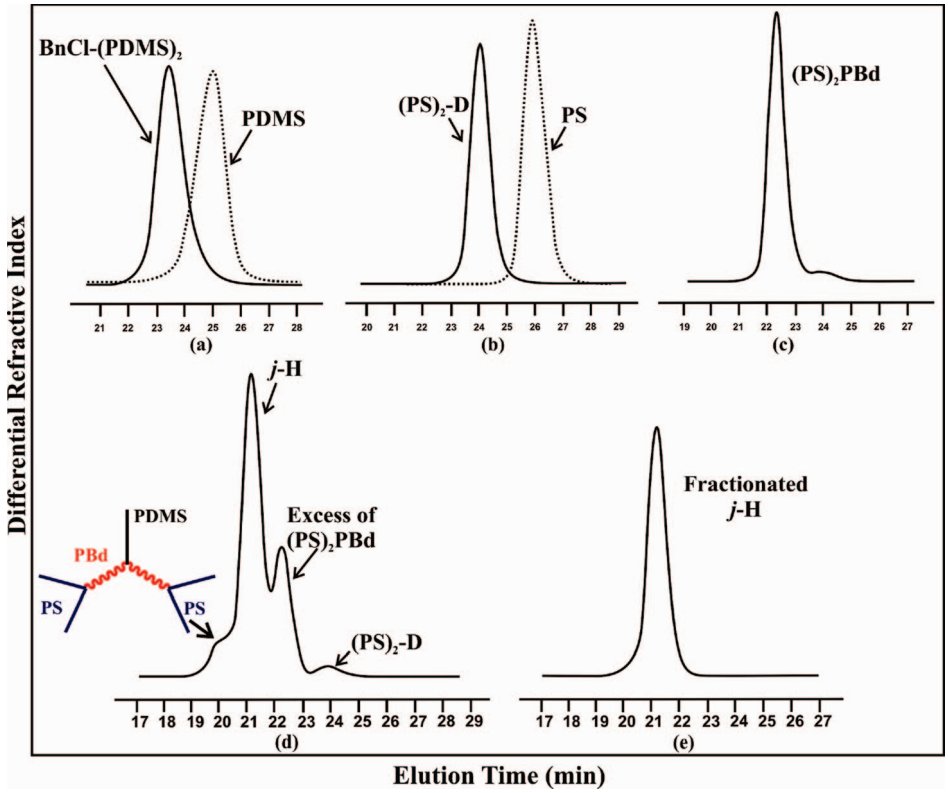

Figure 2. Monitoring the synthesis of Janus-H copolymers (sample *j*-H #2) by SEC: (a) living PDMSOLi and macromolecular linking agent BzCl-$(PDMS)_2$, (b) living PSLi and DPE-tipped macromonomer, (c) living star, and *j*-H copolymer before (d) and after (e) fractionation.

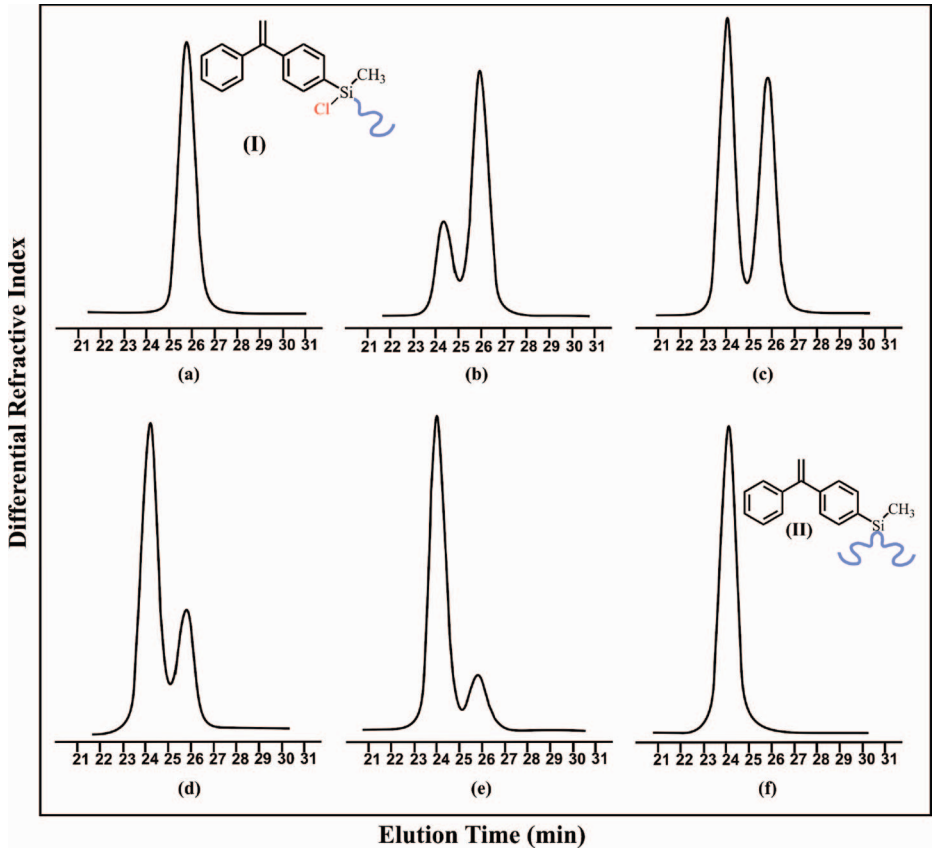

Figure 3. SEC chromatograms during the linking reaction (titration) between linear, living PSLi, and 4-dichloromethylsilyldiphenylethylene (DCMSDPE).

Scheme 4. Metal−Halogen Exchange Reaction

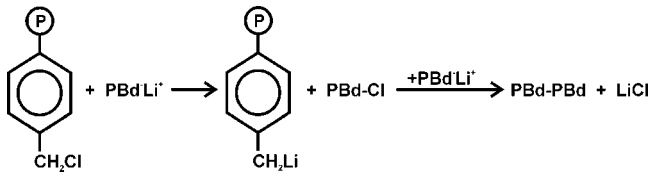

Subsequently, Bd was added, and the polymerization was allowed to proceed for 48 h, leading to the living star copolymer. The higher elution volume peak, observed in only one case (<3%, Figure 2c), corresponds to traces of unreacted $(PS)_2$-D, probably due to incomplete addition of *sec*-BuLi to the double bond.

Finally, the living miktoarm star copolymer $(PS)_2PBd^-Li^+$ was end-capped with DPE and then reacted with BzCl-$(PDMS)_2$ at −78 °C. A 2-fold molar excess of DPE over $(PS)_2PBd^-Li^+$ was used in order to ensure complete end-capping. It was reported[26–31] that the coupling efficiency between living chains and benzyl chloride was fairly low (less than 60%) due to metal−halogen exchange competing with the coupling reaction[32] (Scheme 4). The DPE-end-capping of the living miktoarm star $(PS)_2PBd^-Li^+$ in combination with low temperature (−78 °C) serves to avoid this side reaction.[33] The SEC trace of the reaction product is shown in Figure 2d. No peak corresponding to the dimeric product was observed, indicating the absence of the metal−halogen exchange. The complete lack of any traces of BzCl-$(PDMS)_2$ indicates that the coupling of the living star with the linking agent was quantitative. Furthermore, under these specific conditions the nucleophilic attack of the living polymer at the PDMS chains resulting in cleavage of the Si−O−Si groups[34] was avoided.

The living miktoarm star copolymer reacts with both electrophilic groups, $-Si(Me)Cl_2$ and $-PhCH_2Cl$, of CMPEMDS. As a consequence, the slight excess of the linking reagent resulted in formation of a small amount of a starlike byproduct, as evidenced by the small peak at lower elution volume (Figure 2d).

The isolation of the Janus-H terpolymers (Figure 2e) from the residual intermediates was rather difficult due to the large difference in solubility parameter and surface tension of PDMS and other polymeric chains and fractionation solvents. After examining many solvents/nonsolvent pairs, the hexane/toluene 50/50 mixture was chosen as solvent and methanol as nonsolvent.

The molecular characteristics of the precursors and fractionated Janus-H terpolymers obtained by MO, SEC, SEC-TALLS,

Table 1. Molecular Characteristics of the H-Shaped Terpolymers, *j*-H

	PS		$(PS)_2$-D		$(PS)_2PBd$		PDMS		final terpolymer				
sample	M_w[a] (kg/mol)	I[b] (M_w/M_n)	M_w[a] (kg/mol)	I[b] (M_w/M_n)	M_w[a] (kg/mol)	I[b] (M_w/M_n)	M_n[c] (kg/mol)	I[d] (M_w/M_n)	M_n[e] (kg/mol)	I[b] (M_w/M_n)	% wt PS[f]	% wt PBd[f]	% wt PDMS[f]
j-H #1	18.1	1.02	36.2	1.03	45.6	1.02	20.5	1.07	85.7	1.10	40.6	10.5	48.9
j-H #2	19.5	1.02	39.0	1.02	58.5	1.01	19.2	1.05	96.3	1.03	39.4	19.7	40.9
j-H #3	18.2	1.02	36.4	1.05	76.4	1.02	21.5	1.07	118	1.03	30.3	33.3	36.3

[a] SEC-TALLS in THF at 35 °C. [b] SEC in THF at 30 °C. [c] Calculated from $\{M_{n(final)} - M_{n[(PS)_2PBd]}\}/2$ where $M_{n[(PS)_2PBd]} = M_{w[(PS)_2PBd]}/I$. [d] SEC in $CHCl_3$ at 35 °C. [e] Membrane osmometry in toluene at 35 °C. [f] ^1H NMR in $CDCl_3$.

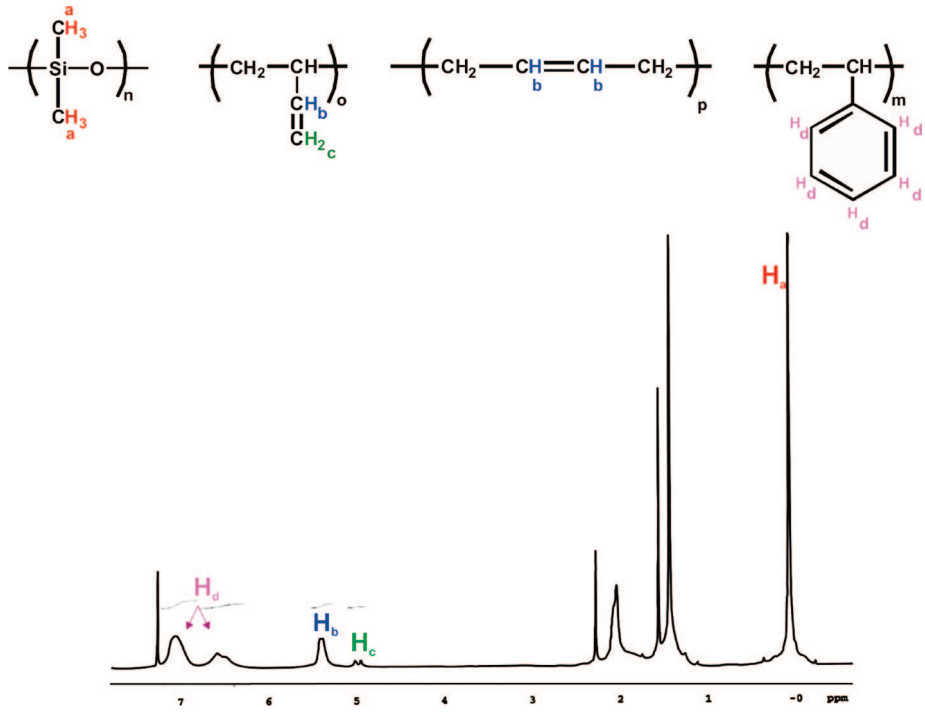

Figure 4. ^{1}H NMR spectrum of sample *j*-H #2 in $CDCl_3$.

Table 2. LALLS Results for the Janus-H Terpolymers in MEK at 25 °C

sample	% of insoluble component	M_w (kg mol^{-1}) of PBd block	$M_{w,mic}$ (kg mol^{-1})	$A_2 \times 10^4$ (mL mol g^{-2})	N_w[a]
j-H #1	10.5	9.4	46.9	3.4	1
j-H #2	19.7	19.5	61.4	2.1	1
j-H #3	33.3	40.0	154	−1.2	2

[a] Calculated from $N_w = M_{w,mic}/M_{w,(PS)_2PBd}$.

and NMR spectroscopy are summarized in Table 1. It is well-known that for block copolymers light scattering leads to apparent M_w values and was thus not used here, especially due to the almost zero refractive index increment of PDMS in THF.

The composition of the final H-shaped terpolymers was obtained from ^{1}H NMR spectra. An example, corresponding to *j*-H #2, is given in Figure 4. The spectrum has all the characteristic peaks of the three different blocks (aromatic protons of PS: 6.3–7.2 ppm; olefin protons of PBd: 5.4 and 5 ppm; and methyl protons of PDMS: ~0 ppm).

The narrow molecular weight distributions of the precursors and the final H-shaped terpolymers indicate a high degree of molecular and compositional homogeneity. This is further supported by the good agreement between the stoichiometric molecular weights and the number-average molecular weights obtained by MO. Moreover, the high degree of compositional homogeneity of the terpolymers is also confirmed by the ^{1}H NMR results, in agreement with the stoichiometric ones.

Micellization Behavior in MEK. The LALLS data of the Janus H-shaped terpolymers in MEK are reported in Table 2, and the representative plots are given in Figure 5. It is clear that samples *j*-H #1 and *j*-H #2 form unimolecular micelles in the concentration range studied (2×10^{-3} g mL$^{-1} < c < 2 \times 10^{-2}$ g mL^{-1}) as is evident from the similar molecular weight values determined in MEK (by LALLS) and THF (by SEC-TALLS). Sample *j*-H #3 shows a very low tendency for aggregation ($N_w = 2$) probably due to the higher molecular weight and content of the insoluble PBd block. In both cases

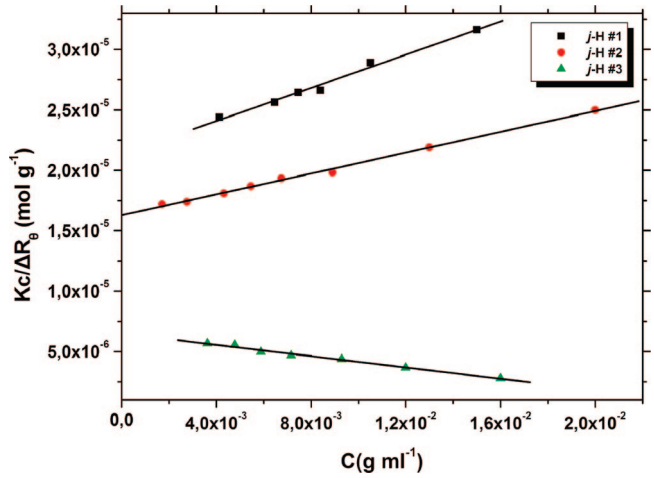

Figure 5. $Kc/\Delta R_\theta$ vs concentration for *j*-H copolymers in MEK at 25 °C.

of unimolecular micelles (samples *j*-H #1 and *j*-H #2) the second virial coefficient A_2 has a positive value, whereas the A_2 in *j*-H #3 was negative due to aggregation.

The conclusions drawn from static light scattering were further supported by dynamic light scattering measurements carried out in both a good (THF) and a selective (MEK) solvent. d*n*/d*c* value of PDMS in THF (~0.005) and MEK (~0.02) are almost zero, rendering the comparison of the results in the two solvents possible. Initially, the hydrodynamic radii of the free terpolymer chains (THF) were obtained at 90° and at 25 °C. Characteristic plots of the concentration dependence of the diffusion coefficient are given in Figure 6, and the results are included in Table 3.

Since THF is a good solvent for all blocks, the analysis of the intensity correlation functions by CONTIN method revealed the existence of only one monodisperse in size population with small dimensions, as expected.

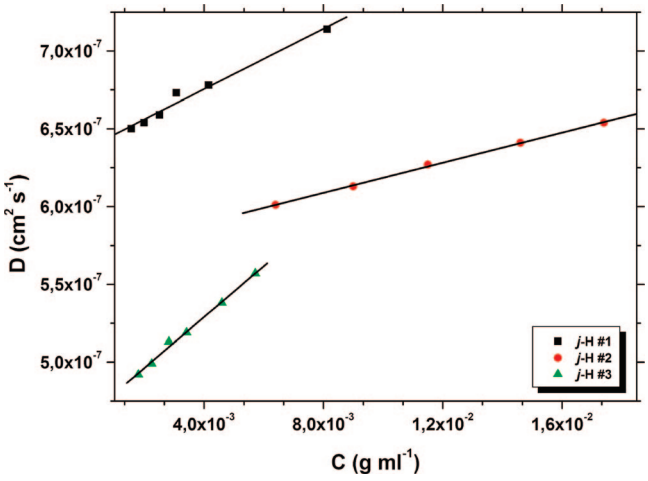

Figure 6. Concentration dependence of apparent diffusion coefficient for *j*-H copolymers in THF at 25 °C.

Table 3. DLS Results for Janus-H Terpolymers in THF at 25 °C

sample	$D_0 \times 10^7$ (cm^2 s^{-1})	k_D (mL g^{-1})	R_h (nm)
j-H #1	6.4	14	7.4
j-H #2	5.7	8.5	8.3
j-H #3	4.6	32	10.2

Table 4. DLS Results for Janus-H Terpolymers in MEK at 25 °C

sample	$D_0 \times 10^7$ (cm^2 s^{-1})	k_D (mL g^{-1})	R_h (nm)	change of R_h with respect to the measurements in THF (%)
j-H #1	9.1	3.8	6.2	−16.2
j-H #2	7.8	6.1	7.3	−12.0
j-H #3	4.3	−35	13.3	+30.4

Next, measurements in MEK, conducted at five different angles (45°, 60°, 75°, 90°, and 120°), revealed negligible angular dependence, the reason all results given correspond to 90° (Table 4, Figure 7). For samples *j*-H #1 and *j*-H #2, CONTIN analysis showed only one narrow peak. The polydispersity factor μ_2/Γ^2, where Γ is the decay rate of the correlation function and μ_2 the second moment of the cumulant analysis, was always lower than 0.1, indicating the presence of monodisperse micelles. The R_h values were lower than those corresponding to THF. Since the difference was greater than the experimental error, the presence of unimolecular micelles

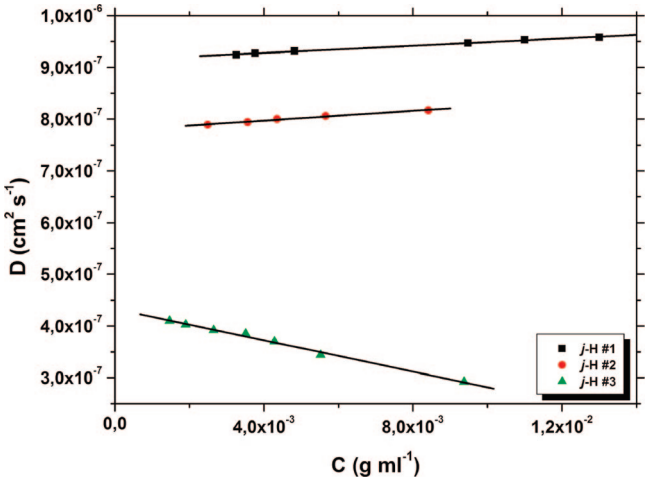

Figure 7. Concentration dependence of apparent diffusion coefficient for *j*-H copolymers in MEK at 25 °C.

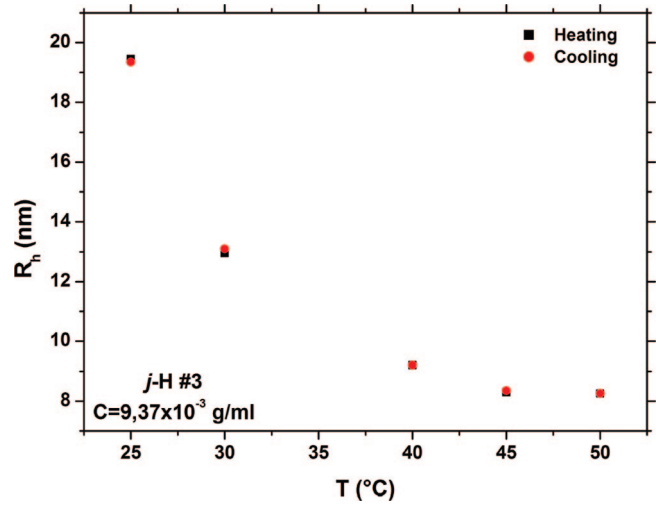

Figure 8. Hydrodynamic radius (R_h) vs temperature for sample *j*-H #3 in MEK ($c = 9.37 \times 10^{-3}$ g mL^{-1}).

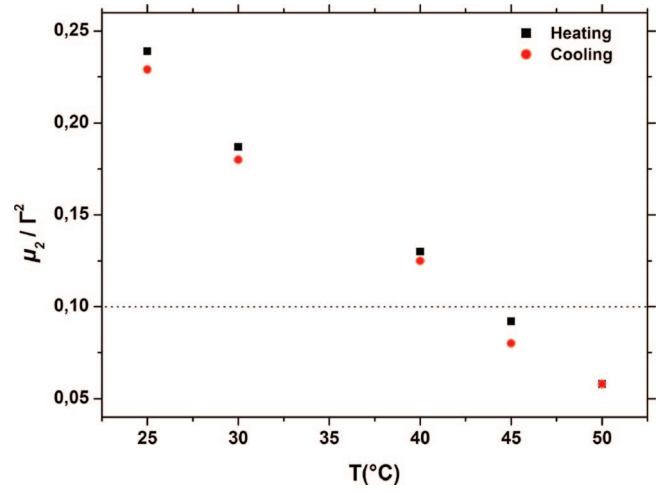

Figure 9. Polydispersity factor (μ_2/Γ^2) vs temperature for sample *j*-H #3 in MEK ($c = 9.37 \times 10^{-3}$ g mL^{-1}).

was confirmed. The difference in hydrodynamic radii is due, on one hand, to the collapse of the inner PBd chains and, on the other, to the smaller dimensions of the PS and PDMS blocks in MEK than in THF.[35] On the contrary, the R_h value for sample *j*-H #3 was higher in MEK than in THF, caused by its slight tendency for aggregation. CONTIN analysis showed one peak characterized by increased polydispersity ($\mu_2/\Gamma^2 > 0.2$). Finally, the negligible angular dependence in association with the small R_h values of the micelles indicates that the structures are almost spherical.

The temperature dependence of the aggregates was also examined. In the case of unimolecular micelles, as was expected, no change in hydrodynamic dimensions was observed upon increasing temperature. On the contrary, the slight tendency for aggregation of sample *j*-H #3 disappeared as soon as energy was provided to the system. As the temperature increased, the peak corresponding to the aggregates was shifted to smaller dimensions, while the polydispersity of the peak gradually decreased. Heating had as a result the "destruction" and convertion of such dimers into unimolecular micelles. The specific phenomenon was reversible and is presented in Figures 8 and 9.

In an attempt to interpret both LALLS and DLS results, we can claim that the lack of aggregation was expected for sample *j*-H #1 due to its smaller insoluble component. Low aggregation degrees could be partly justified from the branched architecture

Scheme 5. Janus-H Copolymer of PS, PBd, and PDMS, *j*-H #2, and Super-H-Shaped Block Copolymer of PS and PI

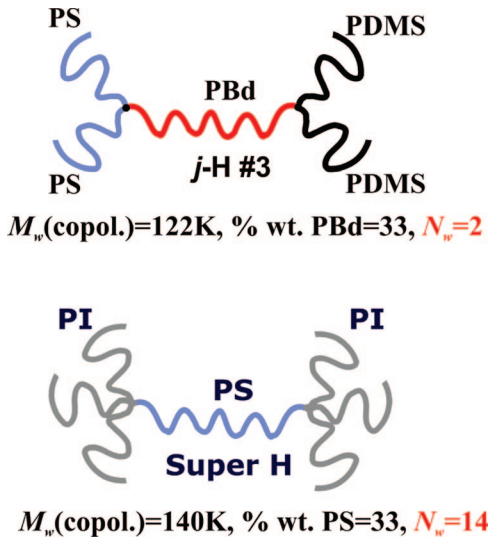

of the samples;[16] however, such a dramatic decrease indicates the existence of an additional parameter that hinders the aggregation. In order to roughly predict the aggregation number of the Janus molecules, a comparison was made between the aggregation results for *j*-H #3 and a super-H PS/PI copolymer synthesized and studied by Iatrou and Hadjichristidis[16] (Scheme 5). This copolymer had similar molecular weight and the same insoluble component content as *j*-H #3. The aggregation number, in a selective solvent for the outer branches (PI), was found to be equal to 14.

Taking into consideration the higher stereochemical hindrance imposed in a super-H architecture (four arms per junction point), we would expect an H-shaped sample like *j*-H #3 to present degrees of aggregation higher than 14 (three arms per junction). A strong incompatibility between PS and PDMS blocks has been observed in the solid state and for a wide range of temperatures[36] and led us to assume that this incompatibility may also occur in solution resulting in some kind of microdomain separation. Since the soluble PS and PDMS blocks are segregated, they act to surround the insoluble PBd blocks, thereby preventing the aggregation of the Janus molecules (Scheme 6).

In an effort to verify the existence of this potential microdomain separation in solution, DLS experiments were conducted in THF for both H-samples (Table 3) and their star-shaped precursors [$(PS)_2$PBd] (Table 5). Since THF is an isorefractive solvent for PDMS, the scattered intensity corresponds only to

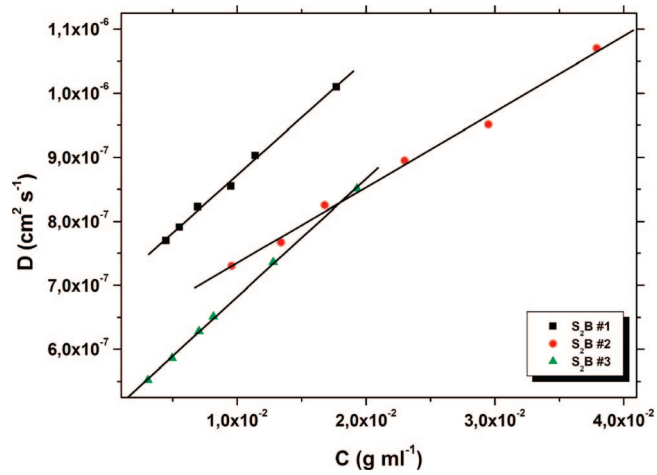

Figure 10. Concentration dependence of apparent diffusion coefficient for $(PS)_2$PBd miktoarm star copolymers in THF at 25 °C.

Table 5. DLS Results for the Star-Shaped Precursors $(PS)_2$PBd (S_2B), in THF at 25 °C

sample	$D_0 \times 10^7$ (cm^2 s^{-1})	k_D (mL g^{-1})	R_h (nm)
S_2B #1	6.9	26	6.9
S_2B #2	6.2	19	7.7
S_2B #3	4.0	37	9.5

the PS/PBd blocks. If the PS and PDMS blocks were segregated, then the measured dimensions would correspond only to the star $(PS)_2$PBd (Scheme 6a). On the contrary, if those two blocks were compatible in solution, the expected dimensions would be higher, since they correspond to the entire terpolymer (Scheme 6b).

As seen in Table 5, the R_h values of the star-shaped precursors (Figure 10, Scheme 6c) are similar to those of the H-shaped polymers, even in the case of sample *j*-H #1 which contains almost 50% of PDMS. The above confirms the existence of some kind of segregation of PS and PDMS in MEK.

Conclusions

A_2BC_2 Janus H-shaped terpolymers, where A is PDMS, B is PBd, and C is PS, were synthesized, for the first time, by using anionic polymerization high-vacuum techniques and two linking agents, CMPEMDS and DCMSDPE. Our methodology involves the linking reaction of BzCl-$(PDMS)_2$, prepared from PDMSOLi and CMPEMDS, with the living miktoarm star copolymer [$(PS)_2$PBd-DPH$^-$Li$^+$]. The synthesis of the living star was achieved by (a) the selective reaction of the PSLi with the two

Scheme 6. Graphical Representation of the Hydrodynamic Volume of (a) *j*-H Copolymer with Separated PS and PDMS Blocks in THF, (b) *j*-H Copolymer with Mixed PS and PDMS Blocks in THF, and (c) Star-Shaped Precursors $(PS)_2$PBd in THF

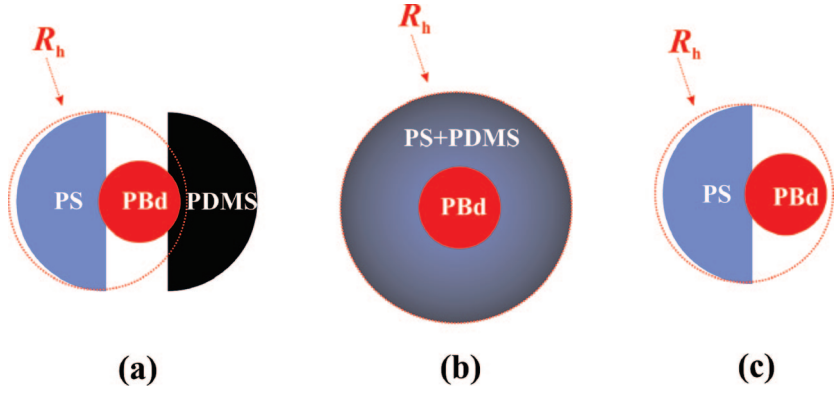

chlorines of DCMSDPE, (b) the addition of *sec*-BuLi to the double bond of the DPE, and (c) the polymerization of Bd. All precursors, intermediates, and final products exhibited very low polydispersity indices, controlled molecular weights, and homogeneity, as indicated by combined characterization analysis. Furthermore, the aggregation properties of the synthesized Janus H-shaped terpolymers were studied by dynamic and static light scattering in MEK, a selective solvent for the outer blocks PDMS and PS. The complexity of the architecture along with "microdomain separation" phenomena, also observed, led to the formation of unimolecular or dimeric aggregates.

References and Notes

(1) Gabor, H.; Ober, C. K. In *Microelectronics Technology. Polymers for Advanced Imaging and Packaging*; ACS Symposium Series 614; American Chemistry Society: Washington, DC, 1995; Chapter 19, p 281.
(2) Zilliox, J. G.; Roovers, J.; Bywater, S. *Macromolecules* **1975**, *8*, 573–578.
(3) Clarson, S. J.; Dodgson, K.; Semlyen, J. A. *Polymer* **1985**, *26*, 930–934.
(4) Bellas, V.; Iatrou, H.; Hadjichristidis, N. *Macromolecules* **2000**, *33*, 6993–6997.
(5) Fragouli, P. G.; Iatrou, H.; Hadjichristidis, N. *J. Polym. Sci., Part A: Polym. Chem.* **2004**, *42*, 514–519.
(6) Fragouli, P. G.; Iatrou, H.; Hadjichristidis, N.; Sakurai, T.; Hirao, A. *J. Polym. Sci., Part A: Polym. Chem.* **2006**, *44*, 614–619.
(7) Fragouli, P. G.; Iatrou, H.; Hadjichristidis, N.; Sakurai, T.; Matsunaga, Y.; Hirao, A. *J. Polym. Sci., Part A: Polym. Chem.* **2006**, *44*, 6587–6599.
(8) Oranli, L.; Bahadur, P.; Riess, G. *Can. J. Chem.* **1985**, *63*, 2691–2695.
(9) Bahadur, P.; Sastry, N; V.; Marti, S.; Riess, G. *Colloids Surf.* **1985**, *16*, 337–346.
(10) Gallot, Y.; Franta, P.; Rempp, P.; Benoit, H. *J. Polym. Sci., Part C* **1964**, *4*, 473–478.
(11) Periard, J.; Riess, G. *Eur. Polym. J.* **1973**, *9*, 687–696.
(12) Selb, J.; Gallot, Y. *Makromol. Chem.* **1980**, *182*, 1491–1498.
(13) Higgins, J. S.; Dawkins, J. V.; Maghami, G. G.; Shakir, S. A. *Polymer* **1986**, *27*, 931–936.
(14) Plestil, J.; Baldrian, J. *Makromol. Chem.* **1975**, *176*, 1009–10028.
(15) Pispas, S.; Hadjichristidis, N.; Potemkin, I.; Khokhlov, A. *Macromolecules* **2000**, *33*, 1741–1746.
(16) Iatrou, H.; Willner, L.; Hadjichristidis, N.; Halperin, A.; Richter, D. *Macromolecules* **1996**, *29*, 581–581.
(17) Iatrou, H.; Hadjichristidis, N.; Meier, G.; Frielinghaus, H.; Monkenbusch, M. *Macromolecules* **2002**, *35*, 5426–5437.
(18) Zhu, Y.; Gido, S. P.; Moshakou, M.; Iatrou, H.; Hadjichristidis, N.; Park, S.; Chang, T. *Macromolecules* **2003**, *36*, 5719.
(19) Hadjichristidis, N.; Iatrou, H.; Pispas, S.; Pitsikalis, M. *J. Polym. Sci., Part A: Polym. Chem.* **2000**, *38*, 3211–3234.
(20) Orfanou, K.; Iatrou, H.; Lohse, D.; Hadjichristidis, N. *Macromolecules* **2006**, *39*, 4361–4365.
(21) Mavroudis, A.; Hadjichristidis, N. *Macromolecules* **2006**, *39*, 535–540.
(22) Thomas, S. In *Organic Synthesis, "The Role of Boron and Silicon"*; Oxford University Press: New York, 1991; p 47.
(23) Liu, Q.; Wilson, G.; Davis, R.; Riffle, J. *Polymer* **1993**, *34*, 3030–3036.
(24) Bellas, V.; Iatrou, H.; Pitsinos, E.; Hadjichristidis, H. *Macromolecules* **2001**, *34*, 5376–5378.
(25) Vazaios, A.; Hadjichristidis, N. *J. Polym. Sci., Part A: Polym. Chem.* **2005**, *43*, 1038–1048.
(26) Altares, T., Jr.; Wyman, D. P.; Allen, V. R.; Meyerson, K. J. *J. Polym. Sci., Part A* **1965**, *3*, 4131–4151.
(27) Fujimoto, T.; Narukawa, H.; Nagasawa, M. *Macromolecules* **1970**, *3*, 57.
(28) Candau, F.; Franta, E. *Makromol. Chem.* **1971**, *149*, 41–50.
(29) Pannell, J. *Polymer* **1971**, *12*, 558–578.
(30) Takaki, M.; Asami, R.; Ichikawa, M. *Macromolecules* **1977**, *10*, 850–855.
(31) Roovers, J. *Polymer* **1979**, *20*, 843–849.
(32) Takaki, M.; Asami, R.; Kuwata, Y. *Polym. J.* **1979**, *11*, 425–431.
(33) Gauthier, M.; Möller, M. *Macromolecules* **1991**, *24*, 4548–4553.
(34) Fujimoto, T.; Zhang, H.; Kazama, T.; Isono, Y. *Polymer* **1992**, *33*, 2208–2213.
(35) Brandrup, J.; Immergut, E. H.; Gruke, E. A. *Polymer Handbook*, 4th ed.; Wiley-Interscience: New York, 1999.
(36) Shefelbine, T. A.; Vigild, M. E.; Matsen, M. W.; Hajduk, D. A.; Hillmyer, M. A.; Cussler, E. L.; Bates, F. S. *J. Am. Chem. Soc.* **1999**, *121*, 8457–8465.

MA702605W